

## Vortex-antivortex annihilation dynamics in a square mesoscopic superconducting cylinder

Edson Sardella,<sup>1</sup> Paulo Noronha Lisboa Filho,<sup>1</sup> Clécio C. de Souza Silva,<sup>2</sup>  
Leonardo Ribeiro Eulálio Cabral,<sup>2</sup> and Wilson Aires Ortiz<sup>3</sup>

<sup>1</sup>*Departamento de Física, Faculdade de Ciências, UNESP–Universidade Estadual Paulista,  
Caixa Postal 473, 17033-360 Bauru, SP, Brazil*

<sup>2</sup>*Departamento de Física, Universidade Federal de Pernambuco, 50670-901 Recife, PE, Brazil*

<sup>3</sup>*Departamento de Física, Universidade Federal de São Carlos, 13565-905 São Carlos, SP, Brazil*  
(Received 11 February 2009; revised manuscript received 16 April 2009; published 17 July 2009)

The dynamics of the annihilation of a vortex-antivortex pair is investigated. The pair is activated magnetically during the run of a simulated hysteresis loop on a square mesoscopic superconducting cylinder with an antidot inserted at its center. We study the nucleation of vortices and antivortices by first increasing the magnetic field, applied parallel to the axis of the sample, from zero until the first vortex is created. A further increase in the field pulls the vortex in, until it reaches the antidot. As the polarity of the field is reversed, an antivortex enters the scene, travels toward the center of the sample, and eventually the pair is annihilated. Depending on the sample size, its temperature, and Ginzburg-Landau parameter, the vortex-antivortex encounter takes place at the antidot or at the superconducting sea around it. The position and velocity of the vortex and antivortex singularities were evaluated as a function of time. The current density, magnetization, and order-parameter topology were also calculated.

DOI: [10.1103/PhysRevB.80.012506](https://doi.org/10.1103/PhysRevB.80.012506)

PACS number(s): 74.78.Na, 74.20.De, 74.25.-q

Achieving a deep understanding of the nucleation and propagation of vortices in real superconductors is a truly complex task, since these entities interact with almost everything: first, with the surface of the specimen, to surpass it; upon entrance, with other vortices that might have already penetrated, and also with defects, which might attract them and even act as pinning centers. Additional difficulties to emulate the problem arise from the fact that vortices generate heat while propagating, what can be harmful to the robustness of the superconducting properties, if not catastrophic, as is the case of vortex avalanches observed in some superconducting films.<sup>1–6</sup> It is quite common, however, that the existence of pinning potentials represent a beneficial feature, since vortices can thus be prevented from undergoing dissipative motion. An interesting approach to the problem, which enables one to address most specificities without excessive complexity, is to work in the small universe of mesoscopic samples. In such an ambient, one can accommodate the essential ingredients: relatively important surface-to-volume ratio, only a few vortices on scene, and a number of defects—the so-called antidots—usually arranged in a regular pattern. Furthermore, one can study the interaction of an individual vortex-antivortex (V-AV) pair and, eventually, witness their mutual annihilation.

Recently, there have been many studies about V-AV configurations in mesoscopic superconductors (see for instance Refs. 7–11). The authors of these references have found that vortices and antivortices may coexist in equilibrium in configurations which look like a V-AV molecule. A somewhat common approach is to assume an *a priori* configuration and minimize the free energy in terms of some relevant parameter for which the V-AV molecule is a stable configuration. Here, we will focus in a rather different approach concerning more with the dynamics of a V-AV encounter. The aim of the present work is to elucidate the details involved in the process of creation of pairs, following their time evolution and ultimate disappearance. We opted to do this making no use of

*a priori* assumptions regarding symmetries, but simply varying the applied magnetic field, allowing for the spontaneous nucleation of a vortex and, cycling the field, of an antivortex, which form a pair of interacting entities, whose subsequent time evolution is monitored.

In this Brief Report we present the dynamics of the annihilation of a V-AV pair activated magnetically during a short hysteresis loop. The geometry we consider is a square mesoscopic superconducting cylinder with an antidot placed at its center. Simulations are made in the presence of an applied magnetic field parallel to the axis of the cylinder. We study the nucleation of vortices and antivortices by first increasing the magnetic field from zero until the first vortex is created. The field was then decreased toward negative values. During this process the vortex travels heading the center of the sample, is trapped by the antidot and is then annihilated by an antivortex as the polarity of the applied field is reversed. To monitor the whole process, we evaluate the position and velocity of the vortex and antivortex singularities as a function of time. We also calculate the order-parameter topology, the current density, and the magnetization. In order to follow the dynamics of the physical quantities we use the gauge-invariant time-dependent Ginzburg-Landau (TDGL) equations. These equations describe the time evolution of the complex order parameter  $\psi$  and the vector potential  $\mathbf{A}$ , which is related to the local magnetic field through the expression  $\mathbf{h} = \nabla \times \mathbf{A}$ . In dimensionless units these equations are given by

$$\left(\frac{\partial}{\partial t} + i\phi\right)\psi = -(-i\nabla - \mathbf{A})^2\psi + (1 - T)\psi(1 - |\psi|^2),$$

$$\beta\left(\frac{\partial \mathbf{A}}{\partial t} + \nabla\phi\right) = \mathbf{J}_s - \kappa^2 \nabla \times \mathbf{h}, \quad (1)$$

where the supercurrent density is

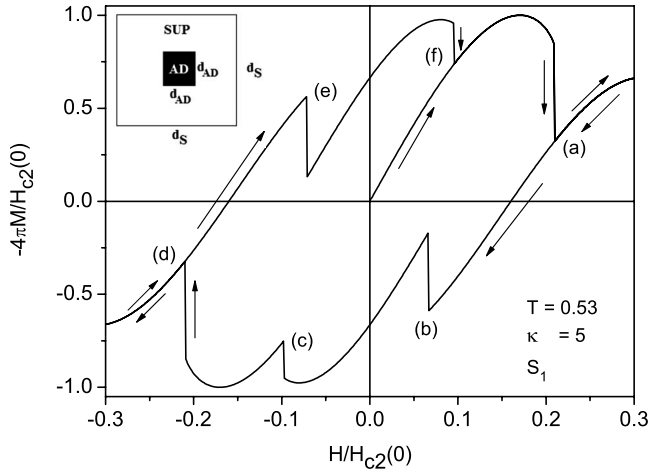


FIG. 1. The magnetization curve normalized to its maximum value as a function of the external applied magnetic field. The meaning of the points marked in the figure are explained in the text. The arrows indicate the direction of the hysteresis loop. The inset illustrates the geometry of the problem.

$$\mathbf{J}_s = (1 - T)\mathcal{R}[\psi^*(-i\nabla - \mathbf{A})\psi]. \quad (2)$$

Here, the distances are measured in units of the coherence length at zero temperature  $\xi(0)$ ; the magnetic field is in units of the upper critical field at zero temperature  $H_{c2}(0)$ ; the temperature is in units of the critical temperature  $T_c$ ; the time is in units of the characteristic time  $t_0 = \pi\hbar/8K_B T_c$ ;  $\kappa$  is the Ginzburg-Landau parameter;  $\beta$  is the relaxation time of the vector potential and is related to the conductivity; and  $\phi$  is the scalar potential. Notice that Eqs. (1) and (2) are gauge invariant since they do not change under the transformation  $\bar{\psi} = \psi e^{i\chi}$ ,  $\bar{\mathbf{A}} = \mathbf{A} + \nabla\chi$ , and  $\bar{\phi} = \phi - \partial\chi/\partial t$ . We choose the zero-scalar potential gauge, that is,  $\bar{\phi} = 0$  at all times. We have solved the TDGL equations upon using the link-variables method.<sup>13–15</sup> Since we consider invariance of the system along the  $z$  direction, our approach could only be applied to a square mesoscopic superconducting cylinder. However, it might also be used for a very thin superconducting film of thickness  $d$ , provided that the effective penetration length  $\Lambda = 2\lambda^2/d$  is larger than the lateral dimensions  $L$  of the film.<sup>16,17</sup> In this scenario, the  $z$  component of the magnetic field outside the film is nearly the same as the applied magnetic field, so the demagnetization factor can be neglected. The dimensions of the samples used in the present work are within this limit.<sup>18</sup> The geometry we have considered is depicted at the top left corner of Fig. 1: the lateral sizes are  $d_S$  for the sample and  $d_{AD}$  for the antidot.

For the study presented in this paper, the relaxation time is kept fixed at  $\beta = 1$ . The GL parameter was also maintained at  $\kappa = 5$ . For  $T = 0.53$ , Fig. 1 shows a short hysteresis loop which was made for a mesoscopic superconducting square (hereafter referred to as sample  $S_1$ ) of dimensions  $d_S = 12$ , with a small antidot at the center, with size  $d_{AD} = 2$ . Points marked with letters, (a), ..., (f), indicate the values of  $H$  where a vortex (antivortex) either enters or exits the sample. The magnetic field is increased from zero until a value somewhat above that at which the first two vortices penetrate in

(a). It is then reversed until the opposite value is achieved and then reversed once more. At point (d), two antivortices penetrate the superconductor. Points (b) and (e) correspond to the exit of a vortex and an antivortex, respectively, immediately after which one flux quantum still remains in the antidot. The point we will be mainly focusing on is (c) [or, equivalently, (f)]. This point corresponds to the entrance of an antivortex, which will encounter a vortex trapped in the antidot. The V-AV pair will annihilate either inside or outside the antidot.

We have made a systematic study of the V-AV annihilation process, varying the experimentally accessible relevant parameters:  $T$ ,  $d_S$ , and  $d_{AD}$ . The other parameters were kept fixed as specified above.

We turn now into a brief discussion of our results. First, we found that for  $d_S$  and  $d_{AD}$  fixed, the V-AV annihilation occurs at a limited temperature interval. Above the upper limit of such interval, the vortex trapped at the antidot leaves the sample before the entrance of the antivortex, and no collision can possibly occur. For the sample  $S_1$  this upper threshold is somewhat above  $T = 0.53$ . As a matter of fact, since the penetration length increases as the temperature approaches  $T_c$ , the supercurrent density associated with the pinned vortex spreads to distances large enough to reach the external border of the sample. This enhances an attractive interaction between the surface and the trapped vortex, facilitating its escape.

At a given temperature, there is a minimum width of the superconducting frame to allow for a V-AV collision outside the antidot. For example, for  $T = 0.23$  and  $d_{AD} = 2$  the minimum size of the frame<sup>19</sup> is 6 (these dimensions define sample  $S_2$ :  $d_S = 8$  and  $d_{AD} = 2$ ). Our reasoning is as follows: the antivortex nucleated at the external border is kept pinned by the surface barrier at the external border while, in turn, the vortex remains pinned at the antidot. Both entities attract each other and the interaction is larger for smaller superconducting frames. It is then easier to pull the vortex out of the antidot for shorter distances. On the other hand, if the superconductor width is increased, the antivortex starts its excursion toward the center before the V-AV attraction becomes appreciable. Being thus less anchored by the surface, the antivortex travels all the way to the antidot and the annihilation process completes there. In support to this argument, Fig. 2 depicts the values of the  $x$  component of the supercurrent density at the surfaces  $y = 12$  and  $y = 8$  for both samples  $S_1$  and  $S_2$ , respectively. These values of  $J_{sx}$  were calculated in the absence of applied field,  $H = 0$ , and thus represent the supercurrent due *only* to the vortex inside the antidot. The V-AV attraction (Lorentz force) will be proportional to  $J_{sx}$ . Notice that, for both samples, the absolute value of  $J_{sx}$  is maximum at the center of the square edge. One can clearly see that, in the middle of the sample edge,  $x = d_S/2$ , the intensity of the Lorentz force is larger for the sample  $S_2$  than for  $S_1$ .

Figure 3 shows the dynamics of the V-AV collision for the sample  $S_1$  at  $T = 0.53$ . Immediately after entering the sample, only the antivortex is in the superconducting sea. As it moves forward to the antidot, at some instant the trapped vortex will come out and both will collide and annihilate.

Another interesting characteristic we have found was that

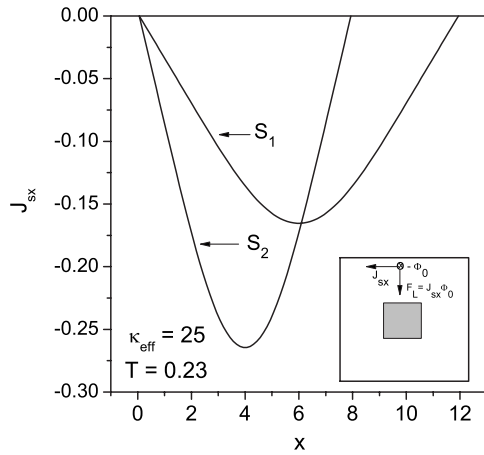


FIG. 2. The supercurrent density along the top surface of the superconductor. The parameters used are specified in the figure. The inset shows the Lorentz force on the antivortex due to the vortex in the antidot.

as the antivortex penetrates, its interaction with the vortex is so strong that both appear entirely deformed. Usually, vortices look like a composition of core surrounded by whirling supercurrents. However, when the vortex and the antivortex approach one another while still partially pinned at the corresponding surfaces, they become elongated, as if squashed, and form a narrow channel between the external surface and the antidot. This can be seen in Fig. 4, which represents the topology of the order parameter  $\psi$  and the supercurrent distribution at the very moment when the collision takes place for the sample  $S_1$  at  $T=0.53$ . Very recently, Gurevich and

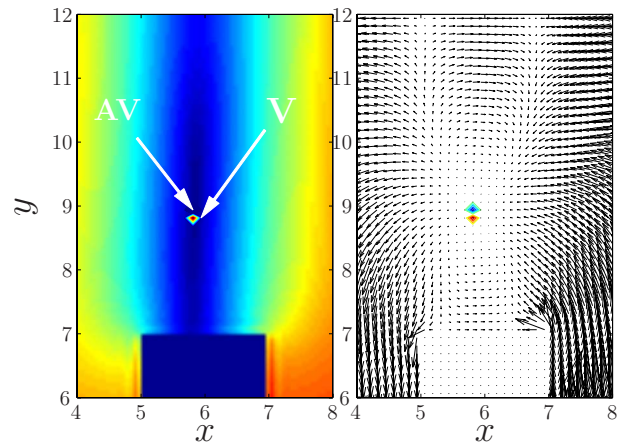


FIG. 4. (Color online) The absolute value of the order parameter (left) and the supercurrent distribution (right) for the sample  $S_1$ ; very dark color means order parameter is very depreciated. The size of the arrows (right) are not real; they were enlarged for better viewing.

Ciovati<sup>20</sup> have studied a V-AV collision in a semi-infinite sample in the context of rf fields. However, they were not able to observe the dramatic deformation of the V-AV cores since their analysis is based on rigid circular-shaped vortex cores.

We also have estimated the instantaneous velocity of the vortex on its way from nucleation at the surface through its capture by the antidot [point (a) of Fig. 1]. In addition, the velocities of both the antivortex entering the sample and that of the vortex exiting the antidot, on their route to annihilation

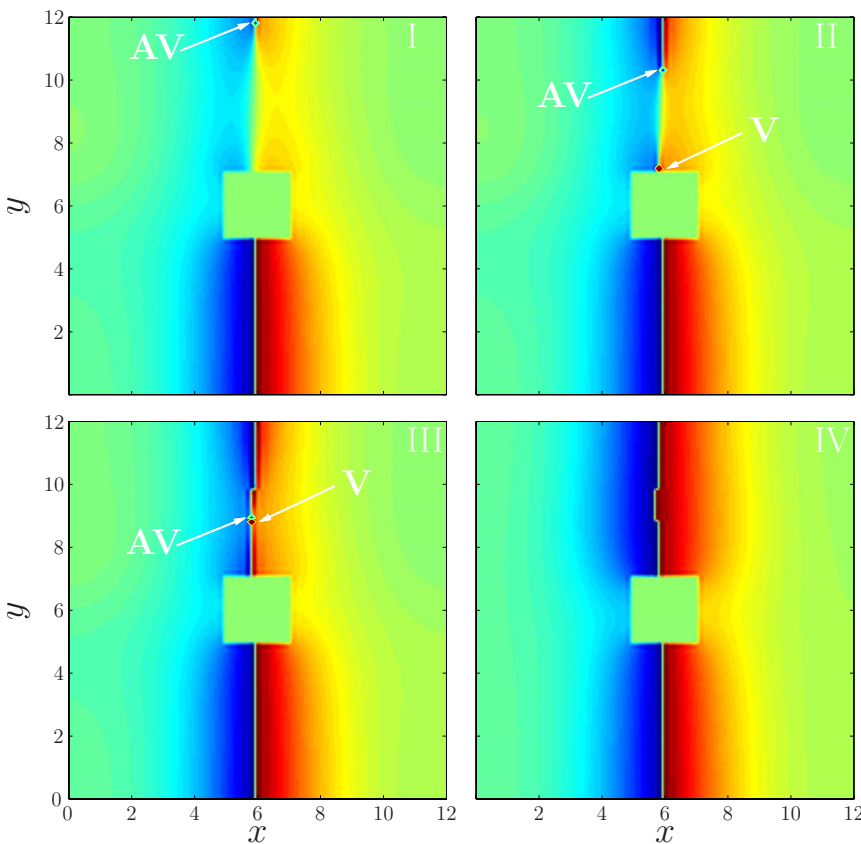


FIG. 3. (Color online) The pictures show the topological shape of the phase of the order parameter; the phase goes from  $-\pi$  (blue/dark gray) to  $\pi$  (red/mid gray). The last picture (IV) corresponds to the stationary state of point (c) of the hysteresis loop of Fig. 1.

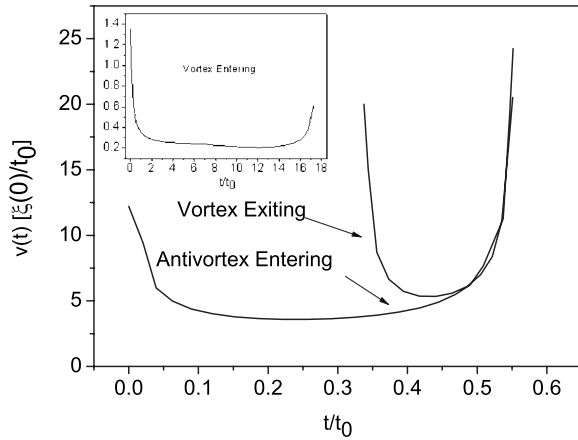


FIG. 5. The modulus of the velocity of the vortex and the anti-vortex for the sample  $S_1$  at  $T=0.53$  as a function of time [point (c) of Fig. 1]; the inset corresponds to point (a).

[point (c) of Fig. 1], were also determined. The results are shown in Fig. 5. It is clearly seen that the velocities achieved during the collision process are much larger than those of a vortex penetrating the sample (at least one order of magnitude, as shown in the inset).

As we have observed previously, during the V-AV collision the order parameter is very small along a straight line but is zero only at two distinct points. The oscillations of the order parameter connected by these two singularities are usually called *kinematic vortices* and it was proposed in Ref. 21 and experimentally observed by Sivakov *et al.*<sup>22</sup> In this last reference it was estimated that a kinematic vortex can achieve a velocity  $v_{kv} \approx 10^5$  m/s which is two orders of

magnitude higher than the velocity of an Abrikosov vortex  $v_{Av} \approx 10^3$  m/s. On the other hand, the velocity of a kinematic vortex is two orders of magnitude smaller than that of a Josephson vortex  $v_{Jv} \approx 10^7$  m/s. For the sample  $S_1$ , the window during which the antivortex remains visible is  $\Delta t = 0.5517t_0$  and the distance it travels is  $\Delta y = 2.875\xi(0)$ ; inserting  $T_c = 3.72$  K and  $\xi(0) = 230$  nm (the relevant parameters for Sn, which were used by Sivakov *et al.*<sup>22</sup>), the average velocity is  $v_{AV} = 1.5 \times 10^5$  m/s. On the other hand, for the vortex exiting the antidot we obtain  $\Delta t = 0.2135t_0$  and  $\Delta y = 1.625\xi(0)$ ; which gives  $v_{Vs} = 2.2 \times 10^5$  m/s. Thus, the velocities involved in the annihilation process are very similar to those of kinematic vortices. It is worth noticing that the large velocities anticipated for the V-AV pair along the collision process, are similar to those developed during the early stage of a vortex avalanche, as observed by the authors of Ref. 6, who reported velocities as large as  $1.8 \times 10^5$  m/s for avalanches in YBCO films. Very recently, Berdiyrov *et al.*<sup>23</sup> have investigated the activation of a kinematic vortex by using a transport current along a superconducting stripe, obtaining experimental results very close to our estimates.

For the vortex first entering the antidot we found an average velocity slightly larger than that for a regular Abrikosov vortex:  $\Delta t = 17.2792t_0$ , and  $\Delta y = 4.125\xi(0)$ , which yields  $v_{Ve} = 6.8 \times 10^3$  m/s. This somewhat larger value—although in the same order of magnitude—might be attributed to the additional attraction exerted by the antidot.

#### ACKNOWLEDGMENTS

The authors thank the Brazilian Agencies FAPESP, FACEPE, and CNPq for financial support.

- <sup>1</sup>C. A. Duran, P. L. Gammel, R. E. Miller, and D. J. Bishop, Phys. Rev. B **52**, 75 (1995).
- <sup>2</sup>P. Leiderer, J. Boneberg, P. Brull, V. Bujok, and S. Herminghaus, Phys. Rev. Lett. **71**, 2646 (1993).
- <sup>3</sup>T. H. Johansen *et al.*, Supercond. Sci. Technol. **14**, 726 (2001).
- <sup>4</sup>F. Colauto, E. M. Choi, J. Y. Lee, S. I. Lee, V. V. Yurchenko, T. H. Johansen, and W. A. Ortiz, Supercond. Sci. Technol. **20**, L48 (2007).
- <sup>5</sup>F. Colauto, E. J. Patino, M. G. Blamire, and W. O. Ortiz, Supercond. Sci. Technol. **21**, 045018 (2008).
- <sup>6</sup>B. Biehler, B. U. Runge, P. Leiderer, and R. G. Mints, Phys. Rev. B **72**, 024532 (2005); B. U. Runge, U. Bolz, J. Eisenmenger, and P. Leiderer, Physica C **341-348**, 2029 (2000).
- <sup>7</sup>G. R. Berdiyrov, M. V. Milošević, and F. M. Peeters, Phys. Rev. Lett. **96**, 207001 (2006).
- <sup>8</sup>R. Geurts, M. V. Milošević, and F. M. Peeters, Phys. Rev. Lett. **97**, 137002 (2006).
- <sup>9</sup>V. R. Misko, V. M. Fomin, J. T. Devreese, and V. V. Moshchalkov, Phys. Rev. Lett. **90**, 147003 (2003).
- <sup>10</sup>A. S. Mel'nikov, I. M. Nefedov, D. A. Ryzhov, I. A. Shereshevskii, V. M. Vinokur, and P. P. Vysheslavtsev, Phys. Rev. B **65**, 140503(R) (2002).
- <sup>11</sup>L. F. Chibotaru, A. Ceulemans, V. Bruyndoncx, and V. V. Moshchalkov, Nature (London) **408**, 833 (2000).

- <sup>12</sup>N. R. Weethamer, in *Superconductivity*, edited by R. D. Parks (Marcel Dekker Inc., New York, 1969).
- <sup>13</sup>W. D. Gropp, H. G. Kaper, G. K. Leaf, D. M. Levine, M. Palumbo, and V. M. Vinokur, J. Comput. Phys. **123**, 254 (1996).
- <sup>14</sup>G. C. Buscaglia, C. Bolech, and A. López, in *Connectivity and Superconductivity*, edited by J. Berger and J. Rubinstein (Springer, Heidelberg, 2000).
- <sup>15</sup>E. Sardella, A. L. Malvezzi, P. N. Lisboa-Filho, and W. A. Ortiz, Phys. Rev. B **74**, 014512 (2006).
- <sup>16</sup>E. H. Brandt, Phys. Rev. B **72**, 024529 (2005).
- <sup>17</sup>D. J. Priour and H. A. Fertig, Phys. Rev. B **67**, 054504 (2003).
- <sup>18</sup>The condition  $\Lambda/L < 1$  is equivalent to  $2\kappa^2 > Ld(1-T)$  in dimensionless units.
- <sup>19</sup>While changing sample and antidot sizes, we have always adopted unitary steps.
- <sup>20</sup>A. Gurevich and G. Ciovati, Phys. Rev. B **77**, 104501 (2008).
- <sup>21</sup>A. Andronov, I. Gordion, V. Kurin, I. Nefedov, and I. Shereshevsky, Physica C **213**, 193 (1993).
- <sup>22</sup>A. G. Sivakov, A. M. Glukhov, A. N. Omelyanchouk, Y. Koval, P. Müller, and A. V. Ustinov, Phys. Rev. Lett. **91**, 267001 (2003).
- <sup>23</sup>G. R. Berdiyrov, M. V. Milošević, and F. M. Peeters, Phys. Rev. B **79**, 184506 (2009).